International Journal of Bifurcation and Chaos, Vol. 22, No. 12 (2012) 1250294 (10 pages)

DOI: 10.1142/S021812741250294X

ANALYTICAL APPROXIMATION OF HETEROCLINIC BIFURCATION IN A 1:4 RESONANCE

ABDELHAK FAHSI
University Hassan II-Mohammadia, FSTM, Mohammadia, Morocco

MOHAMED BELHAQ
Laboratory of Mechanics, University Hassan II-Casablanca, Morocco

Received August 18, 2011; Revised March 29, 2012

Bifurcation of heteroclinic cycle near 1:4 resonance in a self-excited parametrically forced oscillator with quadratic nonlinearity is investigated analytically in this paper. This bifurcation mechanism leads to the disappearance of a slow flow limit cycle giving rise to frequency-locking near the resonance. The analytical approach used to approximate the bifurcation is based on a collision criterion between the slow flow limit cycle and saddles involved in the bifurcation. The amplitudes of the 1:4-subharmonic solution and the slow flow limit cycle are approximated using a double perturbation procedure and the heteroclinic bifurcation is captured applying the collision criterion. For validation, the analytical results are compared to those obtained by numerical simulations.

Keywords: Heteroclinic connection; collision criterion; 1:4 resonance; frequency-locking; double perturbation technique.

1. Introduction

Heteroclinic bifurcation in forced and self-excited nonlinear oscillators occurs near q-subharmonic resonances when pairs of saddles form connections resulting from the disappearance of a limit cycle. All connections appear simultaneously due to the Z_q-symmetry. This bifurcation gives rise to frequency-locking phenomenon between the frequency of limit cycle and the frequency of q-subharmonic response. Such a bifurcation mechanism usually occurs when the system exhibits bistability in which two stable states coexist.

Heteroclinic connections near the 1:4 resonance is a complicated bifurcation problem and only a conjecture near this resonance is given; a rigorous proof is still incomplete [Arnold, 1977]. In contrast, this bifurcation near the other strong 1:q resonances with $q = 1, 2, 3$ is well established [Arnold, 1977]. The problem of approximating heteroclinic bifurcation of cycles near 1:4 resonance is usually tackled by using numerical simulations. For instance, [Berezovskaia & Khibnik, 1981] constructed 1:4 resonance heteroclinic bifurcation curves in the normal form equation using numerical integration. Also, heteroclinic bifurcations near the 1:4 resonance have been analyzed numerically for a nonlinear parametric oscillator using the fourth-order Runge–Kutta method [Belhaq *et al.*, 1986; Belhaq, 1992a] or applying continuation techniques [Krauskopf, 1995; Takens, 2001] on the normal form equation [Arnold, 1977; Takens, 2001]. Recently, a detailed numerical path-following and simulation was carried out to analyze bifurcation to heteroclinic cycles in three and four coupled phase oscillators [Ashwin *et al.*, 2008].

While heteroclinic bifurcations for cycles have been extensively studied numerically, analytical treatment of these bifurcations, on the other hand, are still unexplored. In a recent paper [Belhaq & Fahsi, 2010], the so-called collision criterion was used to approximate a heteroclinic bifurcation near the 1:3 resonance in a self-excited nonlinear oscillator subjected to external forcing. The analytical approximation was in accordance with the result obtained by numerical integration. Motivated by this finding, the present work aims at gaining insight into the potential application of the collision criterion to capture heteroclinic bifurcation near 1:4 resonance. In this context, following a similar strategy as in the 1:3 resonance case [Belhaq & Fahsi, 2010], we first approximate the amplitudes of 1:4 subharmonic solution and the slow flow limit cycle, and then we apply the collision criterion between the two solutions. It is worthy to notice that this criterion was successfully applied to capture homoclinic and heteroclinic bifurcations in two- and three-dimensional autonomous systems [Belhaq *et al.*, 1999; Belhaq *et al.*, 2000; Belhaq & Lakrad, 2000]. In particular, it was rigourously shown that the collision criterion which is accessible via approximations of limit cycles is equivalent to the Melnikov method aiming directly on the separatrices [Belhaq *et al.*, 2000]. In other words, it was concluded that the collision criterion coincides with the Melnikov method when using the Jacobian elliptic functions.

In the next section, we apply the Bogolioubov–Mitropolsky technique [Bogolioubov & Mitropolsky, 1962] to approximate the amplitude–frequency response near the 1:4 resonance. Then, the multiple scales method [Nayfeh & Mook, 1979] is performed on the slow flow to approximate the amplitude of the limit cycle. In Sec. 3, the collision criterion is implemented and approximation of the 1:4 heteroclinic connection is obtained. For validation, the analytical finding is compared with the numerical simulation using phase portraits. The last section concludes the work.

2. 1:4 Subharmonic and Slow Flow Limit Cycle

The system we consider that produces the heteroclinic connection in the 1:4 resonance is a self-excited parametrically forced oscillator with a quadratic nonlinearity given in the dimensionless form as

$$\ddot{x} + \omega_0^2(1 + h\cos\omega t)x - (\alpha - \beta x)\dot{x} - cx^2 = 0, \tag{1}$$

where ω_0 is the natural frequency, α, β are the damping coefficients, c is the quadratic nonlinear component and h, ω are, respectively, the amplitude and frequency of the parametrical excitation. Equation (1) is the classical nonlinear van der Pol–Mathieu oscillator that can model various physical and mechanical phenomena [Nayfeh & Mook, 1979]. The quadratic nonlinear component is useful for testing perturbation methods and can also model various phenomena in the physical and engineering sciences [Mickens, 1996, 2004]. While saddle-node bifurcation has been studied near the 1:4 resonance for Eq. (1) [Belhaq, 1992b], the investigation of 1:4 heteroclinic bifurcation is still unexplored from an analytical view point. It is worth noticing that two possible 1:4 heteroclinic bifurcations exist. Namely, a *trifle* heteroclinic connection formed around the trivial equilibrium and a *clover* heteroclinic connection surrounding both trivial and nontrivial equilibria. All connections appear simultaneously due to the Z_4-symmetry.

An analytical method is performed here to approximate the *trifle* heteroclinic bifurcation near the 1:4 resonance. To do so, we analyze the dynamic near this resonance by setting the resonance condition as

$$\omega_0^2 = \left(\frac{\omega}{4}\right)^2 + \sigma, \tag{2}$$

where σ is a detuning parameter.

To analyze this case we need to order the linear damping and the detuning parameters so that they appear at the second order in the perturbation scheme; the other parameters are ordered at the first order. In other words, we let

$$\begin{gathered} h = \varepsilon h, \quad \beta = \varepsilon\beta, \quad c = \varepsilon c, \\ \alpha = \varepsilon^2\alpha, \quad \sigma = \varepsilon^2\sigma, \end{gathered} \tag{3}$$

where ε is a small bookkeeping parameter. Substituting (2) and (3) into (1) yields

$$\ddot{x} + \left(\frac{\omega}{4}\right)^2 x = \varepsilon\left\{cx^2 - \beta x\dot{x} - h\left(\frac{\omega}{4}\right)^2 x\cos\omega t\right\} + \varepsilon^2\{-\sigma x + \alpha\dot{x}\} + \varepsilon^3\{-h\sigma x\cos\omega t\}. \tag{4}$$

Using the method of Bogolioubov–Mitropolsky [Belhaq & Fahsi, 1997], we expand the solution of (4) up to the third order as

$$x(t) = r\cos\left(\frac{\omega}{4}t+\theta\right) + \varepsilon U_1(r,\theta,t) + \varepsilon^2 U_2(r,\theta,t) + \varepsilon^3 U_3(r,\theta,t), \tag{5}$$

where the amplitude r and the phase θ are governed by the slow flow system

$$\begin{aligned}\frac{dr}{dt} &= \varepsilon A_1(r,\theta) + \varepsilon^2 A_2(r,\theta) + \varepsilon^3 A_3(r,\theta)\\ \frac{d\theta}{dt} &= \varepsilon B_1(r,\theta) + \varepsilon^2 B_2(r,\theta) + \varepsilon^3 B_3(r,\theta).\end{aligned} \tag{6}$$

Introducing $\psi = \frac{\omega}{4}t + \theta$, substituting (5) and (6) into (4), expanding and equating coefficients of like powers of ε, we obtain at different orders

- Order ε^1:

$$\frac{\partial^2 U_1}{\partial t^2} + \left(\frac{\omega}{4}\right)^2 U_1 = cr^2\cos^2\psi + \beta r^2\left(\frac{\omega}{4}\right)\cos\psi\sin\psi - h\left(\frac{\omega}{4}\right)^2 r\cos\psi\cos\omega t + \frac{\omega}{2}A_1\sin\psi + \frac{\omega}{2}rB_1\cos\psi. \tag{7}$$

- Order ε^2:

$$\begin{aligned}\frac{\partial^2 U_2}{\partial t^2} + \left(\frac{\omega}{4}\right)^2 U_2 &= -\sigma r\cos\psi - \alpha r\left(\frac{\omega}{4}\right)\sin\psi + \left(2cr\cos\psi + \beta r\left(\frac{\omega}{4}\right)\sin\psi - h\left(\frac{\omega}{4}\right)^2\cos\omega t\right)U_1\\ &\quad - \beta r\cos\psi\left(A_1\cos\psi - rB_1\sin\psi + \frac{\partial U_1}{\partial t}\right) + \left(\frac{\omega}{2}A_2 + rA_1\frac{\partial B_1}{\partial r}\right.\\ &\quad \left. + rB_1\frac{\partial B_1}{\partial \theta} + 2A_1B_1\right)\sin\psi + \left(\frac{\omega}{2}rB_2 + rB_1^2 - A_1\frac{\partial A_1}{\partial r} - B_1\frac{\partial A_1}{\partial\theta}\right)\cos\psi.\end{aligned} \tag{8}$$

- Order ε^3:

$$\begin{aligned}\frac{\partial^2 U_3}{\partial t^2} + \left(\frac{\omega}{4}\right)^2 U_3 &= -h\sigma r\cos\psi\cos\omega t - \sigma U_1 + \alpha\left(A_1\cos\psi - rB_1\sin\psi + \frac{\partial U_1}{\partial t}\right)\\ &\quad + \left(2cr\cos\psi + \beta r\left(\frac{\omega}{4}\right)\sin\psi - h\left(\frac{\omega}{4}\right)^2\cos\omega t\right)U_2\\ &\quad - \beta r\cos\psi\left(A_2\cos\psi - rB_2\sin\psi + \frac{\partial U_2}{\partial t} + A_1\frac{\partial U_1}{\partial r} + B_1\frac{\partial U_1}{\partial\theta}\right)\\ &\quad + cU_1^2 - \beta U_1\left(A_1\cos\psi - rB_1\sin\psi + \frac{\partial U_1}{\partial t}\right) - \frac{\partial U_1}{\partial r}\left(A_1\frac{\partial A_1}{\partial r} + B_1\frac{\partial A_1}{\partial\theta}\right)\\ &\quad - \frac{\partial U_1}{\partial\theta}\left(A_1\frac{\partial B_1}{\partial r} + B_1\frac{\partial B_1}{\partial\theta}\right) - A_1^2\frac{\partial^2 U_1}{\partial r^2} - B_1^2\frac{\partial^2 U_1}{\partial\theta^2} - 2A_1B_1\frac{\partial^2 U_1}{\partial r\partial\theta}\\ &\quad - 2A_1\frac{\partial^2 U_2}{\partial r\partial t} - 2B_1\frac{\partial^2 U_2}{\partial\theta\partial t} - 2A_2\frac{\partial^2 U_1}{\partial r\partial t} - 2B_2\frac{\partial^2 U_1}{\partial\theta\partial t}\\ &\quad + \left(\frac{\omega}{2}A_3 + rA_1\frac{\partial B_2}{\partial r} + rB_1\frac{\partial B_2}{\partial\theta} + rA_2\frac{\partial B_1}{\partial r} + rB_2\frac{\partial B_1}{\partial\theta} + 2A_1B_2 + 2A_2B_1\right)\sin\psi\\ &\quad + \left(\frac{\omega}{2}rB_2 + 2rB_1B_2 - A_1\frac{\partial A_2}{\partial r} - B_1\frac{\partial A_2}{\partial\theta} - A_2\frac{\partial A_1}{\partial r} - B_2\frac{\partial A_1}{\partial\theta}\right)\cos\psi.\end{aligned} \tag{9}$$

Removing secular terms in these equations and solving them successively, we obtain at different orders of approximations the quantities $A_i(r,\theta)$, $B_i(r,\theta)$ and $U_i(r,\theta,t)$ with $i = 1,2,3$ which are given in the Appendix.

Consequently, the solution up to the third order of (4) is given by

$$x(t) = r\cos\left(\frac{\omega}{4}t + \theta\right) + U_1(r,\theta,t) + U_2(r,\theta,t) + U_3(r,\theta,t) \tag{10}$$

and the slow flow (6) now takes the form

$$\begin{aligned}\frac{dr}{dt} &= Ar - Br^3 - (H_1\sin 4\theta + H_2\cos 4\theta)r^3\\ \frac{d\theta}{dt} &= S - Cr^2 - (H_1\cos 4\theta - H_2\sin 4\theta)r^2,\end{aligned} \tag{11}$$

where $A = \frac{\alpha}{2}$, $B = \frac{2\beta c}{\omega^2}$, $C = \frac{80c^2}{3\omega^3} + \frac{\beta^2}{6\omega}$, $S = \frac{2\sigma}{\omega} + \frac{h^2\omega}{192}$, $H_1 = \frac{h\beta^2}{72\omega} - \frac{20hc^2}{9\omega^3}$ and $H_2 = \frac{h\beta c}{9\omega^2}$.

Nontrivial equilibria of this slow flow, corresponding to 1:4 subharmonic solutions of Eq. (1), are determined by setting $\frac{dr}{dt} = \frac{d\theta}{dt} = 0$. This leads to the amplitude–frequency response equation

$$A_2r^4 + A_1r^2 + A_0 = 0, \tag{12}$$

where $A_2 = B^2 + C^2 - H_1^2 - H_2^2$, $A_1 = -2(AB + SC)$ and $A_0 = A^2 + S^2$.

The phase-frequency response relation reads

$$\tan 4\theta = \frac{(A - Br^2)H_1 - (S - Cr^2)H_2}{(A - Br^2)H_2 + (S - Cr^2)H_1}. \tag{13}$$

Figure 1 depicts the amplitude–frequency response, as given by (12). The solid line denotes the amplitude r_f of stable 1:4 subharmonic solution of (1) corresponding to the four stable equilibria of (11), while the dashed line denotes the amplitude r_s of unstable 1:4 subharmonic solution of (1) corresponding to the saddles of (11).

To test the validity of these analytical approximations, we perform numerical simulations by integrating Eq. (1) using Runge–Kutta method. In Fig. 2, the analytical approximation (10) (solid line) is compared with the numerical result (dotted line) and a good agreement is shown.

On the other hand, periodic motions of the slow flow (11), corresponding to quasiperiodic solution of (1), can be approximated by performing the multiple scale method on the slow flow Cartesian system corresponding to the polar form (11), written as

$$\begin{aligned}\frac{du}{dt} &= Au + Sv - (Bu + Cv)(u^2 + v^2) - H_1v(v^2 - 3u^2) - H_2u(u^2 - 3v^2)\\ \frac{dv}{dt} &= -Su + Av - (Bv - Cu)(u^2 + v^2) + H_1u(u^2 - 3v^2) - H_2v(v^2 - 3u^2),\end{aligned} \tag{14}$$

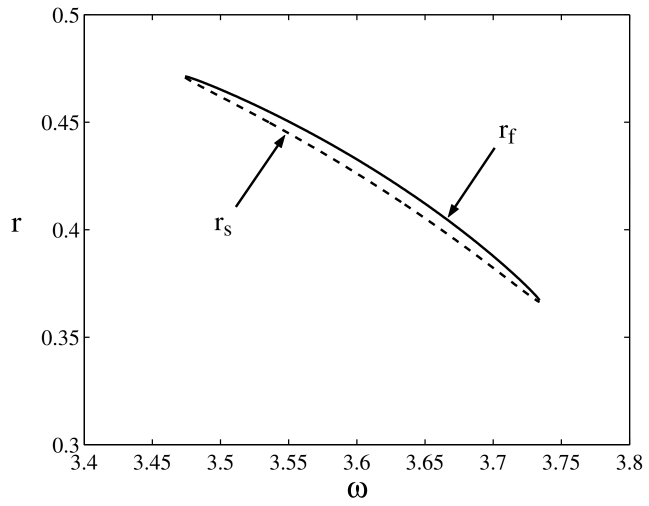

Fig. 1. Amplitude–frequency response curves r_f, r_s near the 1:4 resonance. Solid line for stable and dashed line for unstable, $\omega_0 = 1$, $\alpha = 0.01$, $\beta = 0.2$, $c = 1$, $h = 0.2$.

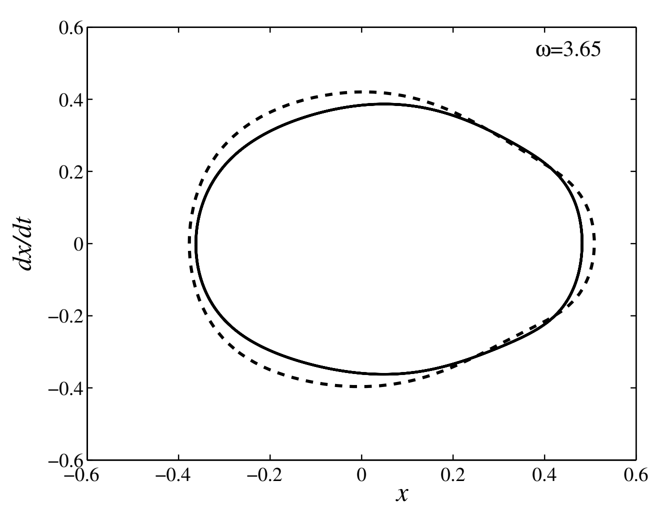

Fig. 2. Comparison between the analytical approximation (10) (solid line) and the numerical integration of (1) (dashed line). Values of parameters are fixed as in Fig. 1.

where $u = r\cos\theta$ and $v = -r\sin\theta$. Following previous works [Belhaq & Fahsi, 2009; Belhaq & Houssni, 1999], a bookkeeping parameter μ is introduced in damping and nonlinearity terms and parameters are scaled in (14) as follows

$$\frac{du}{dt} = Sv + \mu f(u,v),\qquad \frac{dv}{dt} = -Su + \mu g(u,v), \tag{15}$$

where $f(u,v)$ and $g(u,v)$ are given by

$$\begin{aligned} f(u,v) &= Au - (Bu + Cv)(u^2+v^2) \\ &\quad - H_1 v(v^2-3u^2) - H_2 u(u^2-3v^2), \\ g(u,v) &= Av - (Bv - Cu)(u^2+v^2) \\ &\quad + H_1 u(u^2-3v^2) - H_2 v(v^2-3u^2). \end{aligned} \tag{16}$$

Using the multiple scales method, a solution up to the second order of (15) is sought in the form

$$\begin{aligned} u(t) &= u_0(T_0,T_1,T_2) + \mu u_1(T_0,T_1,T_2) \\ &\quad + \mu^2 u_2(T_0,T_1,T_2), \\ v(t) &= v_0(T_0,T_1,T_2) + \mu v_1(T_0,T_1,T_2) \\ &\quad + \mu^2 v_2(T_0,T_1,T_2), \end{aligned} \tag{17}$$

where $T_i = \mu^i t$ $(i = 0,1,2)$. Substituting (17) into (15) and collecting terms, we get at different orders

- Order μ^0:

$$\begin{cases} D_0^2 u_0 + S^2 u_0 = 0, \\ Sv_0 = D_0 u_0. \end{cases} \tag{18}$$

- Order μ^1:

$$\begin{cases} D_0^2 u_1 + S^2 u_1 = -2D_0D_1u_0 + D_0(f(u_0,v_0)) \\ \qquad\qquad + Sg(u_0,v_0), \\ Sv_1 = D_0u_1 + D_1u_0 - f(u_0,v_0). \end{cases} \tag{19}$$

- Order μ^2:

$$\begin{cases} D_0^2u_2 + S^2u_2 = -2D_0D_2u_0 - D_0D_1u_1 - SD_1v_1 + D_0\left(u_1\dfrac{\partial f}{\partial u}(u_0,v_0) + v_1\dfrac{\partial f}{\partial v}(u_0,v_0)\right) \\ \qquad\qquad + S\left(u_1\dfrac{\partial g}{\partial u}(u_0,v_0) + v_1\dfrac{\partial g}{\partial v}(u_0,v_0)\right), \\ Sv_2 = D_0u_2 + D_1u_1 + D_2u_0 - \left(u_1\dfrac{\partial f}{\partial u}(u_0,v_0) + v_1\dfrac{\partial f}{\partial v}(u_0,v_0)\right), \end{cases} \tag{20}$$

where $D_i^j = \frac{\partial^j}{\partial T_i^j}$. A solution to the first order of system (18) is given by

$$\begin{aligned} u_0(T_0,T_1) &= R(T_1)\cos(ST_0 + \varphi(T_1)), \\ v_0(T_0,T_1) &= -R(T_1)\sin(ST_0 + \varphi(T_1)). \end{aligned} \tag{21}$$

Substituting (21) into (19) and removing secular terms, we obtain the following partial differential system on R and φ

$$D_1R = AR - BR^3,\qquad D_1\varphi = -CR^2. \tag{22}$$

The first-order approximate periodic solution of the slow flow (15) reads

$$u(t) = R\cos\nu t,\qquad v(t) = -R\sin\nu t, \tag{23}$$

where the amplitude R and the frequency ν are obtained by setting $\frac{dR}{dt} = 0$ and given, respectively, by

$$R = \sqrt{\frac{A}{B}}, \tag{24}$$

$$\nu = S - CR^2. \tag{25}$$

At the second-order approximation, a particular solution of system (19) is given by

$$\begin{aligned} &u_1(T_0,T_1,T_2) \\ &\quad = \frac{R^3(T_1,T_2)}{4S}(H_1\cos(3ST_0 + 3\varphi(T_1,T_2)) \\ &\qquad - H_2\sin(3ST_0 + 3\varphi(T_1,T_2))), \\ &v_1(T_0,T_1,T_2) \\ &\quad = \frac{R^3(T_1,T_2)}{4S}(H_1\sin(3ST_0 + 3\varphi(T_1,T_2)) \\ &\qquad + H_2\cos(3ST_0 + 3\varphi(T_1,T_2))). \end{aligned} \tag{26}$$

Substituting (21) and (26) into (20) and removing secular terms gives the following partial differential system on R and φ

$$\begin{aligned} D_2R &= 0, \\ D_2\varphi &= -\frac{3R^4}{4S}\left(H_1^2 + H_2^2\right). \end{aligned} \tag{27}$$

Hence, the second-order approximate periodic solution of the slow flow (15) is given by

$$u(t) = R\cos\nu t + \frac{R^3}{4S}(H_1\cos(3\nu t) - H_2\sin(3\nu t)),$$

$$v(t) = -R\sin\nu t + \frac{R^3}{4S}(H_1\sin(3\nu t) + H_2\cos(3\nu t)), \tag{28}$$

where R and ν are now given, respectively, by

$$R = \sqrt{\frac{A}{B}}, \tag{29}$$

$$\nu = S - CR^2 - \frac{3R^4}{4S}\left(H_1^2 + H_2^2\right). \tag{30}$$

Using (28), the modulated amplitude of quasiperiodic solutions of (1) is now approximated by

$$r(t) = \sqrt{R^2 + \frac{R^6}{16S^2}\left(H_1^2 + H_2^2\right) + \frac{2R^4}{4S}(H_1\cos(4\nu t) - H_2\sin(4\nu t))} \tag{31}$$

and the envelope of this modulated amplitude is delimited by $r_{\min}$ and $r_{\max}$ given by

$$r_{\min} = \sqrt{R^2 + \frac{R^6}{16S^2}\left(H_1^2 + H_2^2\right) - \frac{2R^4}{4S}\sqrt{H_1^2 + H_2^2}}, \tag{32}$$

$$r_{\max} = \sqrt{R^2 + \frac{R^6}{16S^2}\left(H_1^2 + H_2^2\right) + \frac{2R^4}{4S}\sqrt{H_1^2 + H_2^2}}. \tag{33}$$

In Fig. 3, we plot the amplitude–frequency response curves r_s and r_f as given by (12), as well as the modulation domain of the amplitude of the slow flow limit cycle $r_{\min}$ and $r_{\max}$ (solid lines), as given by (32) and (33). The comparison between these analytical predictions (solid lines) and the numerical simulations (double circles connected with a vertical dashed line) indicates that, at the leading order, the analytical approximation captures the modulation zone of the quasiperiodic response, especially away from the frequency-locking domain. The figure also indicates that when approaching the small synchronization area numerically (approximately $3.605 < \omega < 3.689$), the upper modulation limit from the left or the lower modulation limit from the right hits the unstable branch producing, respectively, a *trifle* heteroclinic bifurcation or a *clover* heteroclinic bifurcation.

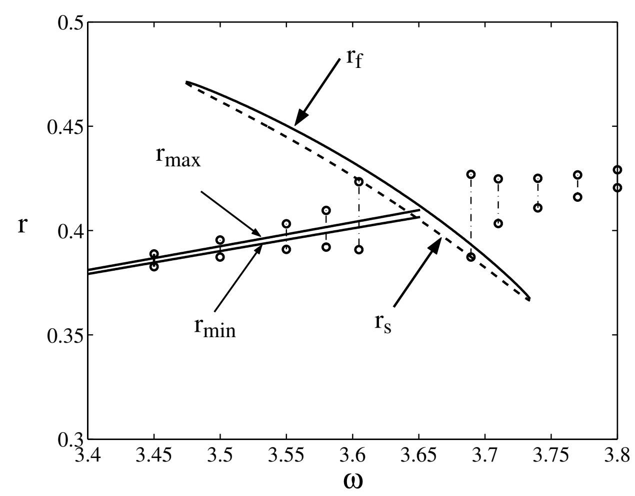

Fig. 3. Amplitude–frequency response r_f, r_s and modulation domain of the amplitude of slow flow limit cycle. Numerical simulation: double circles, analytical approximation: lines $r_{\min}$, $r_{\max}$. Values of parameters are fixed as in Fig. 1.

3. Collision Criterion and Heteroclinic Bifurcation

To approximate analytically the *trifle* heteroclinic bifurcation near the 1:4 resonance, we apply the collision criterion between the slow flow limit cycle and the four saddles. In other words, at the bifurcation the following condition

$$r_{\max} = r_s \tag{34}$$

should be satisfied. Here, $r_{\max}$ is the upper modulation limit of the amplitude of slow flow limit cycle given by (33) and r_s is the saddle stationary solution of the slow flow (11) given by (12).

Figure 4 shows the analytical prediction of the *trifle* heteroclinic connection, plotted by the curve labeled H_a, as given by the criterion (34). This

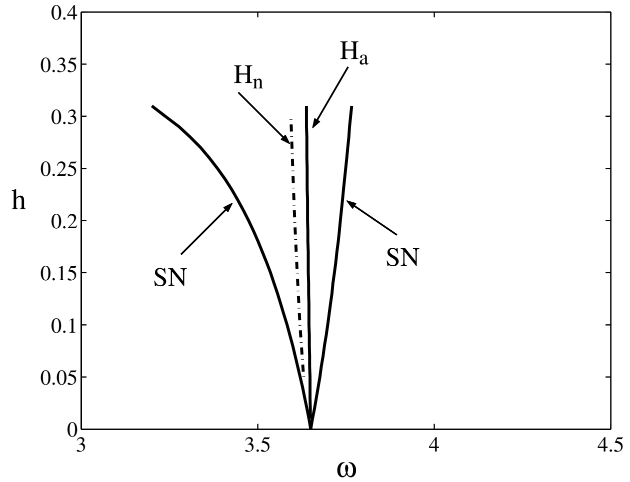

Fig. 4. Bifurcation curves for the 1:4 subharmonic resonance. SN: Saddle-node bifurcation curves, H_a: Analytical *trifle* heteroclinic bifurcation, H_n: Numerical *trifle* heteroclinic bifurcation. Values of parameters are fixed as in Fig. 1.

analytical prediction is compared to the numerical heteroclinic bifurcation curve, labeled H_n, obtained by integrating the slow flow system (14) using the Runge–Kutta method. The comparison shows a good agreement. The analytical curves, labeled SN, obtained from (12) denote the saddle-node bifurcation location delimiting the region where the 1:4 subharmonic cycles exist.

Figure 5 illustrates examples of phase portraits of the slow flow (14) for some values of ω picked from Fig. 3. For values of ω taken far from the resonance, only a slow flow stable limit cycle exists and attracts all initial conditions. A related phase portrait is shown in subfigures (a) and (i) for $\omega = 3.45$ and $\omega = 3.75$, respectively. The subfigures (c) and (g) for $\omega = 3.55$ and $\omega = 3.70$, respectively, indicate the coexistence of two stable states, namely, a cycle of order 4 born by saddle-node bifurcation and a limit cycle. As the forcing frequency varies, the stable slow flow limit cycle approaches the saddles and disappears via a *trifle* or a *clover* heteroclinic connection, as shown in subfigures (d) and (f) for $\omega = 3.6048$ and $\omega = 3.6894$, respectively. This mechanism gives rise to frequency-locking, in which the response of the system follows the 1:4 subharmonic frequency (see subfigure (e) for $\omega = 3.65$).

Note that the stable and unstable cycles of order 4 appear or disappear via saddle-node

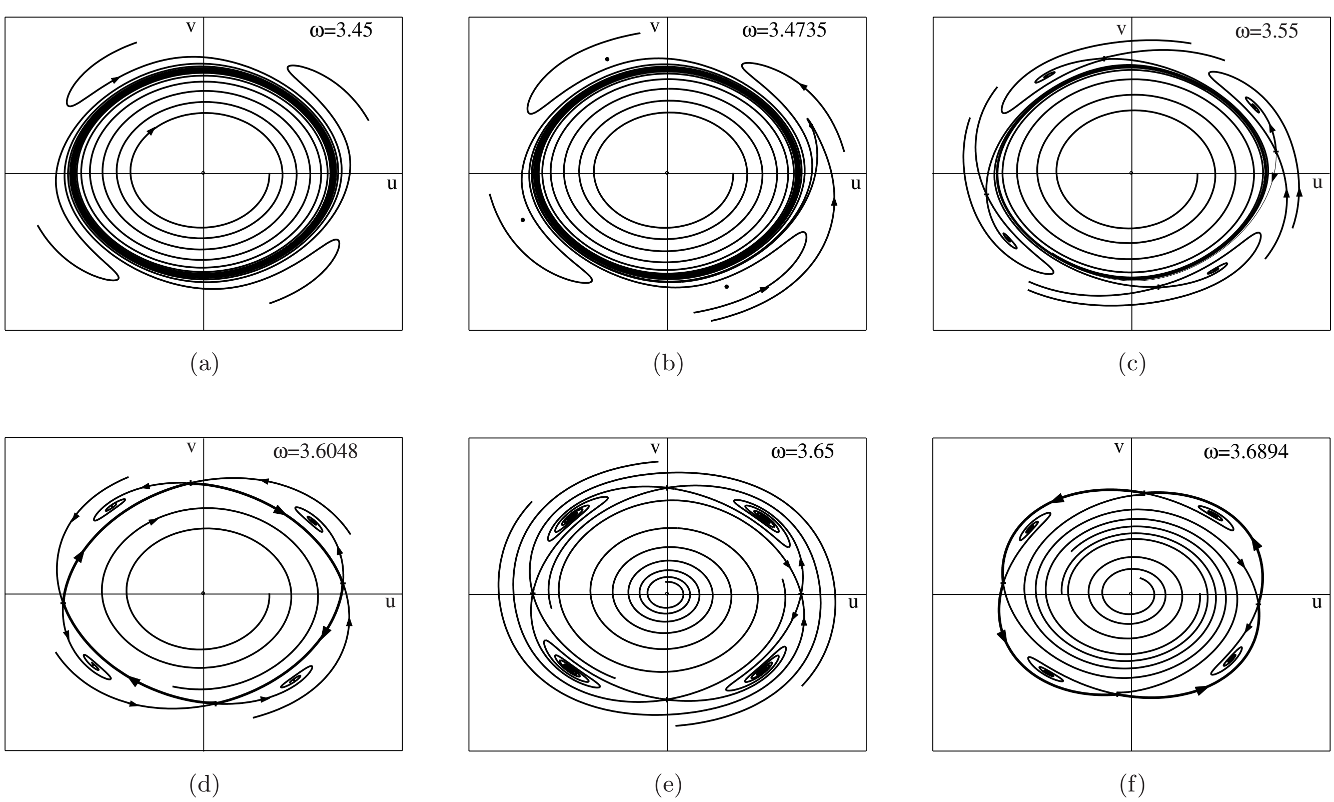

Fig. 5. Examples of phase portraits of the slow flow at different frequencies picked from Fig. 3. (d) *Trifle* connection, (f) *clover* connection, (b) and (h) saddle-node bifurcations. Values of parameters are fixed as in Fig. 1.

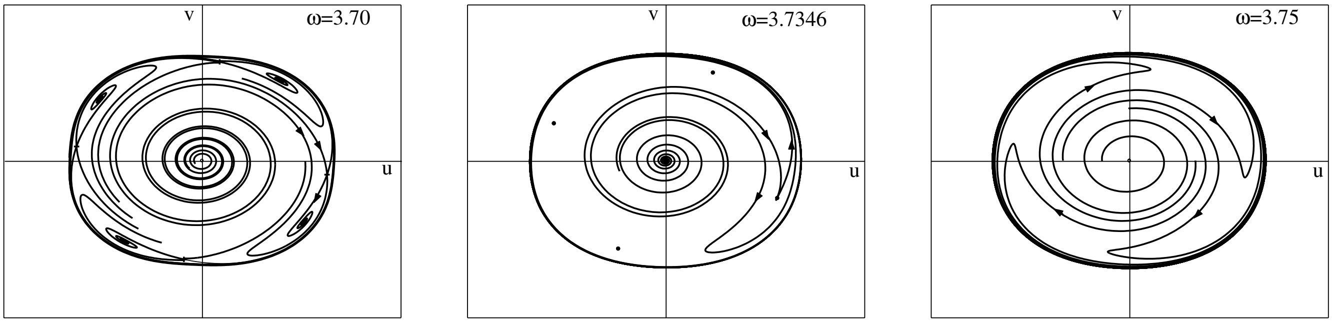

(g) (h) (i)

Fig. 5. (*Continued*)

bifurcations, as shown in subfigures (b) and (h) for $\omega = 3.4735$ and $\omega = 3.7346$, respectively.

We point out that this analytical study focused only on the *trifle* heteroclinic bifurcation corresponding to the case where the limit cycle disappears leaving the stable cycles located outside the *trifle* connection, as shown in Figs. 5(c)–5(e). The other case where the heteroclinic bifurcation leaves the stable cycles inside the *clover* connection ($\omega = 3.6894$) is not considered here [see Figs. 5(e)–5(g)]. In fact, analytical treatment of this later bifurcation requires the construction of an analytical expression of the slow flow limit cycle surrounding all equilibria, which is not easy to tackle.

4. Conclusions

We have studied analytically bifurcation to heteroclinic cycle near a 1:4 resonance in a self-excited parametrically forced oscillator with a quadratic nonlinearity. The analytical approach is based on the collision criterion between the slow flow limit cycle and the slow flow saddles involved in the bifurcation. We have focused our efforts on the investigation of the *trifle* heteroclinic bifurcation in which the limit cycle disappears from inside the connection [Figs. 5(c)–5(e)]. The results show that the analytical approach was able to capture the *trifle* heteroclinic bifurcation of the 1:4 resonance. The comparison of the analytical finding to numerical results show a good agreement indicating that the collision criterion can effectively be exploited to capture heteroclinic bifurcations near 1:4 resonance. In contrast, analytical treatment of the *clover* heteroclinic bifurcation where the limit cycle disappears from outside the connection [Figs. 5(e)–5(g)] presents serious difficulties and requires additional efforts in term of approximating the slow flow limit cycle.

It is worthy to notice that combining the collision criterion with the Jacobian elliptic functions (instead of the trigonometric ones used in the present work) may give a more accurate analytical approximation of the 1:4 resonance heteroclinic connection. Therefore, the principal challenge that emerges from the present study is the problem of approximating analytically the slow flow limit cycle near the heteroclinic bifurcations using the Jacobian elliptic functions. Meeting this challenge may provide an efficient tool to analytically explore bifurcation of heteroclinic cycles near strong resonances.

References

Arnold, V. I. [1977] "Loss of stability of self-oscillation close to resonance and versal deformations of equivariant vector fields," *Funct. Anal. Appl.* **11**, 85–92.

Ashwin, P., Burylko, O. & Maistrenko, Y. [2008] "Bifurcation to heteroclinic cycles and sensitivity in three and four coupled phase oscillators," *Physica D* **237**, 454–466.

Belhaq, M., Clerc, R. L. & Hartmann, C. [1986] "Numerical study for 4-resonance in a forced Liénard equation," *C. R. Acad. Paris* **303**, 873–876 (in French).

Belhaq, M. [1992a] "4-subharmonic bifurcation and homoclinic transition near resonance point in nonlinear parametric oscillator," *Mech. Res. Commun.* **19**, 279–287.

Belhaq, M. [1992b] "Numerical study for 4-resonance in a forced Liénard equation," *C. R. Acad. Paris* **314**, 859–864 (in French).

Belhaq, M. & Fahsi, A. [1997] "Higher-order approximation of subharmonics close to strong resonances in

the forced oscillators," *Int. J. Comp. Math. Appl.* **33**, 133–144.
Belhaq, M. & Houssni, M. [1999] "Quasi-periodic oscillations, chaos and suppression of chaos in a nonlinear oscillator driven by parametric and external excitations," *Nonlin. Dyn.* **18**, 1–24.
Belhaq, M., Lakrad, F. & Fahsi, A. [1999] "Predicting homoclinic bifurcations in planar autonomous systems," *Nonlin. Dyn.* **18**, 303–310.
Belhaq, M., Fiedler, B. & Lakrad, F. [2000] "Homoclinic connections in strongly self-excited nonlinear oscillators: The Melnikov function and the elliptic Lindstedt–Poincaré method," *Nonlin. Dyn.* **23**, 67–86.
Belhaq, M. & Lakrad, F. [2000] "Analytics of homoclinic bifurcations in three-dimensional systems," *Int. J. Bifurcation and Chaos* **12**, 2479–2486.
Belhaq, M. & Fahsi, A. [2009] "Hysteresis suppression for primary and subharmonic 3:1 resonances using fast excitation," *Nonlin. Dyn.* **57**, 275–287.
Belhaq, M. & Fahsi, A. [2010] "Analytics of heteroclinic bifurcation in a 3:1 subharmonic resonance," *Nonlin. Dyn.* **62**, 1001–1008.
Berezovskaia, F. S. & Khibnik, A. I. [1981] "On the bifurcation of separatrices in the problem of stability loss of auto-oscillations near 1:4 resonance," *PMM U.S.S.R.* **44**, 663–667.
Bogolioubov, M. & Mitropolsky, I. [1962] *Les Méthodes Asymptotiques en Théorie des Oscillations Non Linéaires* (Gauthier-Villars, Paris).
Krauskopf, B. [1995] "On the 1:4 resonance problem," PhD thesis, University of Groningen.
Mickens, R. E. [1996] *Oscillations in Planar Dynamic Systems* (World Scientific, Singapore).
Mickens, R. E. [2004] "Quadratic non-linear oscillators," *J. Sound Vib.* **270**, 427–432.
Nayfeh, A. H. & Mook, D. T. [1979] *Nonlinear Oscillations* (Wiley, NY).
Takens, R. [2001] *Global Analysis of Dynamical Systems. Festschrift dedicated to Floris Takens for his 60th Birthday*, eds. Broer, H. W., Krauskopf, B. & Vegter, G. (Taylor and Francis).

Appendix

- Order ε^1:

$$\begin{cases} A_1(r,\theta) = 0, \\ B_1(r,\theta) = 0, \end{cases}$$

$$U_1(r,\theta,t) = \frac{8cr^2}{\omega^2} - \frac{8cr^2}{3\omega^2}\cos\left(\frac{\omega}{2}t + 2\theta\right) - \frac{2\beta r^2}{3\omega}\sin\left(\frac{\omega}{2}t + 2\theta\right) + \frac{hr}{16}\cos\left(\frac{3\omega}{4}t - \theta\right) + \frac{hr}{48}\cos\left(\frac{5\omega}{4}t + \theta\right).$$

- Order ε^2:

$$\begin{cases} A_2(r,\theta) = \dfrac{\alpha}{2}r - \dfrac{2\beta c}{\omega^2}r^3, \\[2ex] B_2(r,\theta) = \dfrac{2\sigma}{\omega} + \dfrac{h^2\omega}{192} - \left(\dfrac{80c^2}{3\omega^3} + \dfrac{\beta^2}{6\omega}\right)r^2, \end{cases}$$

$$\begin{aligned} U_2(r,\theta,t) = {} & -\frac{7hcr^2}{9\omega^2}\cos\left(\frac{\omega}{2}t - 2\theta\right) + \frac{h\beta r^2}{36\omega}\sin\left(\frac{\omega}{2}t - 2\theta\right) + \left(\frac{16c^2}{3\omega^4} - \frac{\beta^2}{2\omega^2}\right)r^3\cos\left(\frac{3\omega}{4}t + 3\theta\right) \\ & + \frac{10\beta cr^3}{3\omega^3}\sin\left(\frac{3\omega}{4}t + 3\theta\right) + \frac{4hcr^2}{9\omega^2}\cos(\omega t) - \frac{2h\beta r^2}{45\omega}\sin(\omega t) - \frac{hcr^2}{21\omega^2}\cos\left(\frac{3\omega}{2}t + 2\theta\right) \\ & - \frac{h\beta r^2}{60\omega}\sin\left(\frac{3\omega}{2}t + 2\theta\right) + \frac{h^2r}{1536}\cos\left(\frac{7\omega}{4}t - \theta\right) + \frac{h^2r}{7680}\cos\left(\frac{9\omega}{4}t + \theta\right). \end{aligned}$$

- Order ε^3:

$$\begin{cases} A_3(r,\theta) = \left(\dfrac{20hc^2}{9\omega^3} - \dfrac{h\beta^2}{72\omega}\right)r^3\sin 4\theta - \dfrac{h\beta c}{9\omega^2}r^3\cos 4\theta, \\[2ex] B_3(r,\theta) = \left(\dfrac{20hc^2}{9\omega^3} - \dfrac{h\beta^2}{72\omega}\right)r^2\cos 4\theta + \dfrac{h\beta c}{9\omega^2}r^2\sin 4\theta. \end{cases}$$

$$
\begin{aligned}
U_3(r,\theta,t) &= \left(\frac{9728c^3}{9\omega^6}+\frac{176\beta^2 c}{9\omega^4}\right)r^4-\left(\frac{3h^2c}{16\omega^2}+\frac{128\sigma c}{\omega^4}+\frac{4\alpha\beta}{\omega^2}\right)r^2\\
&\quad-\left(\left(\frac{15104c^3}{27\omega^6}+\frac{80\beta^2c}{27\omega^4}\right)r^4-\left(\frac{11h^2c}{3024\omega^2}+\frac{128\sigma c}{3\omega^4}-\frac{4\alpha\beta}{9\omega^2}\right)r^2\right)\cos\left(\frac{\omega}{2}t+2\theta\right)\\
&\quad-\left(\left(\frac{2336\beta c^2}{27\omega^5}+\frac{2\beta^3}{27\omega^3}\right)r^4-\left(\frac{121h^2\beta}{8640\omega}+\frac{16\beta\sigma}{3\omega^3}+\frac{64\alpha c}{9\omega^3}\right)r^2\right)\sin\left(\frac{\omega}{2}t+2\theta\right)\\
&\quad-\left(\left(\frac{56hc^2}{9\omega^4}+\frac{h\beta^2}{30\omega^2}\right)r^3-\left(\frac{25h^3}{24576}+\frac{3h\sigma}{2\omega^2}\right)r\right)\cos\left(\frac{3\omega}{4}t-\theta\right)-\frac{7\beta hcr^3}{90\omega^3}\sin\left(\frac{3\omega}{4}t-\theta\right)\\
&\quad+\left(\frac{472\beta^2c}{135\omega^4}-\frac{256c^3}{27\omega^6}\right)r^4\cos(\omega t+4\theta)+\left(\frac{52\beta^3}{135\omega^3}-\frac{1376\beta c^2}{135\omega^5}\right)r^4\sin(\omega t+4\theta)\\
&\quad+\left(\left(\frac{104hc^2}{189\omega^4}-\frac{h\beta^2}{27\omega^2}\right)r^3-\left(\frac{197h^3}{1105920}-\frac{5h\sigma}{18\omega^2}\right)r\right)\cos\left(\frac{5\omega}{4}t+\theta\right)-\frac{61\beta hcr^3}{630\omega^3}\sin\left(\frac{5\omega}{4}t+\theta\right)\\
&\quad-\frac{31h^2cr^2}{2520\omega^2}\cos\left(\frac{3\omega}{2}t-2\theta\right)-\frac{\beta h^2r^2}{2016\omega}\sin\left(\frac{3\omega}{2}t-2\theta\right)+\frac{3\beta hcr^3}{40\omega^3}\sin\left(\frac{7\omega}{4}t+3\theta\right)\\
&\quad+\left(\frac{17hc^2}{189\omega^4}-\frac{61h\beta^2}{4320\omega^2}\right)r^3\cos\left(\frac{7\omega}{4}t+3\theta\right)+\frac{17h^2cr^2}{5670\omega^2}\cos(2\omega t)-\frac{\beta h^2r^2}{1134\omega}\sin(2\omega t)\\
&\quad-\frac{37h^2cr^2}{124740\omega^2}\cos\left(\frac{5\omega}{2}t+2\theta\right)-\frac{\beta h^2r^2}{6480\omega}\sin\left(\frac{5\omega}{2}t+2\theta\right)+\frac{h^3r}{368640}\cos\left(\frac{11\omega}{4}t-\theta\right)\\
&\quad+\frac{h^3r}{2580480}\cos\left(\frac{13\omega}{4}t+\theta\right).
\end{aligned}
$$